Desalination and Water Treatment
www.deswater.com

doi: 10.5004/dwt.2017.20617

74 (2017) 137–148
May

A new approach in simultaneous calibration of Hazen–Williams coefficients and demand of nodes in of water distribution systems

Fariba Sherri[a], Amir Hossein Mahvi[b,*], Abbas Toloie Eshlaghy[c], Amir Hessam Hassani[a]

[a]*Department of Environmental Engineering, Faculty of Environment and Energy, Science and Research Branch, Islamic Azad University, Tehran, Iran, Tel. +989125461588; email: faribasherri@gmail.com (F. Sherri), Tel. +989121039899; email: ahhassani@srbiau.acir (A.H. Hassani)*
[b]*Center for Solid Waste Research, Institute for Environmental Research, Tehran University of Medical Sciences, Tehran, Iran, Tel. +989123211827; email: ahmahvi@yahoo.com*
[c]*Faculty of Management and Economic, Industrial Management Department, Science and Research Branch, Islamic Azad University, Tehran, Iran, Tel. +989123108756; email: toloie@gmail.com*

Received 19 May 2016; Accepted 17 February 2017

ABSTRACT

Calibration is necessary to make models of water distribution systems (WDSs) perform similarly to actual events; however, calibration is often complicated and time-consuming. The present study provides a new approach for simultaneous calibration of Hazen–Williams coefficients and nodal demand using the hydraulic simulator of the WaterGEMS that includes fast messy genetic algorithm as the optimization tool. For WDS calibration, instead of optimization using extended period approach during a day, several hourly optimization problems are considered. This reduces optimization time and computational effort. In the proposed approach, pipes and nodes are classified by physical characteristics such as age and material and topology of the water distribution network. Classification of pipes and nodes makes the decision space smaller and makes it easier to find a solution in a reasonable time. The water distribution network was calibrated at each time step separately, and then, by aggregating the results, an optimal solution was achieved to minimize the difference between the measured performance and simulation results. The validity of the proposed approach was tested for a two-loop network, and its efficiency in complicated cases was evaluated through application to a part of the Tehran WDS. The results show that the proposed method can produce acceptable results in a reasonable time even for large and complicated WDSs. The case study under actual conditions showed that the difference between observed and simulated pressure at all nodes was <2 m and volume of computation decreased to 66.7%.

Keywords: Water distribution systems; Hazen–Williams roughness coefficients; Water demand; Genetic algorithm; Calibration

1. Introduction

Water distribution systems (WDSs) are complex, essential and costly structures in urban areas. The purpose of a WDS is to supply the demand of consumers with enough pressure and at the desired quality [1]. Water pressure management is a way to reduce operating expenses [2]. Given the critical role of water distribution networks (WDNs) in urban areas, the performance of these infrastructures is very important. Several optimization models and techniques have been used to improve WDSs performance [3].

Given that the majority of WDNs are composed of aging pipelines, the redesign and reconstruction of these networks is an undeniable necessity that will entail huge cost for water and wastewater companies. Optimal management of these systems and the related costs makes it necessary to evaluate their current states and determine their main weaknesses. The hydraulic reliability of WDNs can be

* Corresponding author.

increased by implementing optimal and economic plans for reconstruction of networks.

Different evolutionary optimization algorithms have been used in WDS optimization, such as genetic algorithms (GA) [4–6], simulated annealing [7], ant colony optimization (ACO) [8], harmony search [9,10], shuffled frog leaping algorithm [11], scatter search [12] and honey-bee mating optimization [13]. Different objective functions for hydraulic calibration of WDNs have been proposed. Ormsbee and Wood [14] considered the minimum difference between observed and calculated pressure in network nodes as the objective function when adjusting the roughness coefficient of the model. Kumar et al. [15] considered the WDS calibration objective function to minimize the difference between observed and simulated pressure and flow. Parameters such as the roughness coefficient, nodal demand, demand patterns and leakage of nodes as well as water quality coefficients, including the volumetric decline coefficient and the decay of pipe wall coefficient, were the calibration parameters used. Weiwei et al. [16] calibrated a roughness coefficient using the real-coded GA under steady-state conditions. Borzì et al. [17] minimized the difference between the observed and calculated pressure at nodes as well as the difference between the observed and calculated flow of pipes as the objective function of the calibration model. Yu et al. [18] minimized the difference between the observed and calculated pressure at nodes, flow in pipes and water level in the tank as the objective function in calibration process.

Jamasb et al. [19] calibrated the pipe roughness coefficient and nodal demand in a WDS using a GA under the steady-state conditions. Kang and Lansey [20] calibrated the pipe roughness coefficient and nodal demand using the least squares method under the steady-state conditions. Cheng and He [21] calibrated nodal demand in a WDS using sensitivity analysis for extended period. Asadzadeh et al. [22] calibrated pipe roughness and demand pattern coefficients using a GA for extended period. Sanz and Pérez [23] calibrated demand pattern coefficients using the first-order second-moment method based on a linear gradient for extended period. Morosini et al. [24] calibrated the pipe roughness coefficient and nodal demand using a Bayesian algorithm called shuffled complex evolution metropolis (SCEM-UA) for extended period.

Tabesh et al. [1] compared demand-driven and pressure-dependent hydraulic analysis methods for optimal calibration of the WDS under critical conditions using a standard GA. The pipe roughness coefficient, nodal demand and diameter of the pipe were used as calibration variables. They found that the pressure dependent method was more efficient than the demand-driven method. Kang and Lansey [25] reduced the dimensions of the unknowns in a WDS calibration problem by considering the nodal demand with similar patterns as lumped parameters and grouped pipes with similar materials. The calibration parameters considered were nodal demand and pipe roughness.

Dini [26] used an artificial neural network for WDS simulation to increase the computational speed of the optimization algorithms. Dini and Tabesh [27] calibrated the Hazen–Williams and nodal demand pattern coefficients simultaneously using an ACO algorithm. The algorithm was time-consuming for complicated WDNs. The proposed approach in this study for WDS calibration uses the Hazen–Williams coefficient and nodal demand as calibration parameters. The objective function is to minimize the square of the difference between the measured and simulated pressures at junctions in the network.

The pipes and nodes are first classified into groups based on physical conditions such as pipe age and material, land use and population density where the nodes/pipes are located on the network topology. Classification of pipes and nodes decreases the size of the decision space in the calibration process. The 24-h calibration problem is broken into several steady-state problems to reduce the number of evaluations and the time needed to reach an optimal solution. The times selected for steady-state calibration are selected in a way to be representative of changes in system demand for a given demand pattern. Each episode is optimized separately with the fast messy GA (FMGA), and the results are aggregated to achieve a final model parameter that minimizes the calibration objective function. Different method of WDS calibration that proposed in this study is the main innovation of this study. The main difference between this study and previously published studies on WDS calibration is that the 24-h simulation optimization is disaggregated to several steady-state optimization problems to reduce simulation optimization time and computational effort. A method is then proposed for finding the total calibration results based on individual simulations.

2. Materials and methods

Differences in materials and the age of pipes in a WDN and changes in the roughness coefficient as the age of the pipes increase have direct effects on the hydraulics of a WDN. Before planning a WDN, the model must be calibrated based on the roughness coefficient and nodal demand. The objective function is minimizing the difference between the measured and simulated pressures and flows at monitoring points along the WDN. In the proposed approach, the 24-h period of calibration was broken into steady-state calibration problems to reduce the number of calculations and the time needed to reach an optimal solution. The calibration times were representative of variability in system hydraulics. Each time step selected was optimized separately, and the results were aggregated to find a final optimal solution.

2.1. Network calibration

Calibration changes model characteristics and parameters until the simulation results match the values observed during actual system performance as much as possible. The Hazen–Williams coefficients and nodal demand were the adjusting parameters for hydraulic calibration of the WDN. A GA was used to solve the optimization model proposed for calibration. Calibration efficiency was evaluated as how well the simulated pressure and flow in the hydraulic model matched the observed values. The criteria for this purpose is as follows [28]:

$$F = \frac{\sum_{nh=1}^{Nh} W_{nh}\left(\frac{Hsim_{nh} - Hobs_{nh}}{HP_{nt}}\right)^2}{NH} \quad (1)$$

where W_{nh} is the normalized weighting factor of the hydraulic heads. The weighting factor can be calculated as follows [28]:

$$W_{nh} = \frac{Hobs_{nh}}{\sum Hobs_{nh}} \quad (2)$$

$Hobs_{nh}$ is the observed hydraulic head at nh-th point; $Hsim_{nh}$ is the simulated hydraulic head at nh-th point; NH is the number of hydraulic head observations. HP_{nt} notes the hydraulic head per fitness point [28].

Root mean squared error (RMSE) and Nash–Sutcliffe efficiency (NSE) were used to evaluate the results of calibration. The RMSE value that is closest to zero represents the most accurate result. RMSE is calculated as follows:

$$RMSE = \sqrt{\frac{\sum_{i=1}^{n}(Actual_i - Forcast_i)^2}{n}} \quad (3)$$

where n is the number of observations; $Actual_i$ and $Forecast_i$ are the measured and simulated values of the desired variable, respectively (pressure and flow), at point i. The NSE is calculated as follows:

$$NSE = 1 - \frac{\sum(obs - sim)^2}{\sum((obs - mean(obs))^2} \quad (4)$$

where obs and sim are the measured and simulated values of the calibration variables, respectively (pressure and flow), at point i. The NSE that is closest to 1 represents the most desirable results.

2.2. Optimization algorithm

The optimization algorithm used was the FMGA, which is able to increase the rate of convergence by reducing the length of the chromosomes and eliminating unfavorable genes [29]. In the FMGA, the length of the strings (chromosomes) changes from one string to another. Short strings (partial solutions) are produced and evaluated in the first stage of GA optimization. Short strings with higher than the average fitness are preserved in the building blocks to produce better solutions. FMGA begins with an initial population of full-length strings, which are filtered by a building block. FMGA identifies the superior short strings by deleting some genes from the basic strings, and the short identified strings are then used to produce a new solution. Each solution is created using link and cutting operations instead of a standard crossover operator in GA. The cutting operator divides each string into two strings, and the link operator joints two strings to form a unique string. FMGA identifies building blocks and reproduces solutions in a number of foreign repetitions. The generation continues until an optimal solution is found, and the maximum number of iterations is reached. FMGA works like a filter that eliminates undesirable genes; the resulting population includes only short chromosomes with desirable genes. Filtering is continued until all chromosomes are reduced to the desired length. This type of algorithm resists exposure to the local minimum and, thus, can solve problems in a shorter period of time. FMGA is safer from deception than standard GA, and they converge to an optimal answer with incredibly enticing functions [30].

At the onset of optimization, it is important to determine appropriate values for the parameters. In many evolutionary algorithms, such as GA, optimization depends on the parameters used, and the appropriate amount determined. Parameters cannot be precisely determined, and their effect in any particular case may vary [31].

3. Assessment of the proposed model

3.1. Case study #1

The two-loop network proposed by Alperovits and Shamir [32] was used to illustrate the validity of the proposed approach. This network has been often used as a benchmark example [27]. The layout of the network is shown in Fig. 1, and the specifications of the network and demand patterns are shown in Table 1. A hydraulic model of the network was developed by WaterGEMS software, and the pressure of the nodes in the network was simulated for 4, 7, 10, 13, 16, 19, 22 and 24 h of the day. These times are considered representative of times of variation in daily water demand. The pipes were classified into four groups based on their Hazen–Williams coefficients.

After steady-state calibration of the WDN for the selected times using WaterGEMS simulator and FMGA, different Hazen–Williams coefficients were obtained for the pipes. The most-often repeated coefficient in each group was selected as the appropriate roughness coefficient.

3.2. Case study #2

The case study that is focused in this study is a WDN at the west of Tehran, the capital of Iran. The number of pipes and nodes in this network is very high; thus, the network was simplified, and pipes with diameters of <60 mm, which do not perform as main pipes, were omitted from the WDN. The system was then checked to assure that the simplification had not affected the system hydraulics. The simplified WDN consisted of a reservoir, 191 pipes, 137 nodes and 10 pressure relief valves to reduce downstream pressure to 2.5–2.6 atm. The maximum water level of the reservoir was 1,324.21 m. A summary of network pipes characteristics are

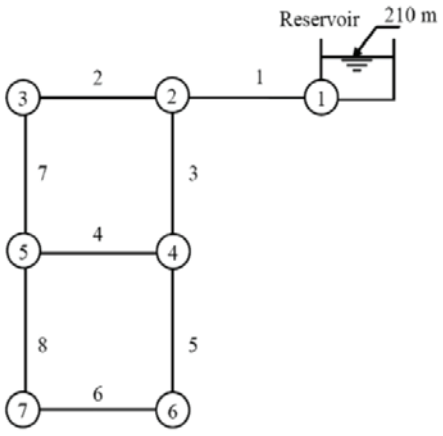

Fig. 1. Two-loop network with eight pipes and seven nodes [32].

Table 1
Two-loop pipe network data [27]

Node characteristics			Pipe characteristics				Demand pattern coefficient					
No.	*E* (m)	BD (L/s)	No.	*L* (m)	*D* (mm)	HW	*T* (h)	*C* (%)	*T* (h)	*C* (%)	*T* (h)	*C* (%)
1	210	0	1	1,000	450	130	1	0.96	9	1.00	17	1.08
2	150	27.8	2	1,000	350	80	2	0.92	10	1.01	18	1.09
3	160	27.8	3	1,000	350	130	3	0.88	11	1.02	19	1.08
4	155	33.4	4	1,000	150	70	4	0.84	12	1.03	20	1.07
5	150	75.0	5	1,000	350	100	5	0.8	13	1.04	21	1.06
6	165	91.7	6	1,000	100	80	6	0.86	14	1.05	22	1.05
7	160	55.6	7	1,000	350	100	7	0.90	15	1.06	23	1.00
			8	1,000	250	70	8	1.06	16	1.07	24	0.98

Table 2
Properties of network pipes

Material	Total length in the considered WDN (m)	Diameter (mm)
Ductile iron	835	60
	1,170	80
	8,052	100
	9,681	150
	8,718	200
	3,263	250
	1,836	300
	1,438	350
	2,290	400
	1,130	500
	1,714	700
Steel	3,547	1,200
	1,345	900
Total	45,019	

shown in Table 2. The population was 113,378, and area encompassed by this portion of the WDN was 659.18 ha. The maximum demand occurs at 1 pm and is 682 L/s. The minimum demand occurs at 4 am and is 361 L/s.

This WDN was considered for improvement by a local organization; thus, it is important to provide a realistic view of current performance. The hydraulic model of this WDN was developed using ArcGIS and WaterGEMS software. The inflow to this WDN was recorded by ultrasonic flow meters for a total of 1 year in 15 min time steps. The inflow was measured by a flow meter (Ultrasonic Flexim, Germany) having an accuracy of ±0.1% and a repeatability of ±0.2%. These observations were used for WDN model calibration. The daily demand pattern for the study area is shown in Fig. 2.

For pressure monitoring, nine logger devices were placed at nine points according to WDN layout as shown in Fig. 3. The data loggers (Sharif Tarasheh, Iran) had an accuracy of ±0.1%. Nodal pressure was measured 24 h/d for

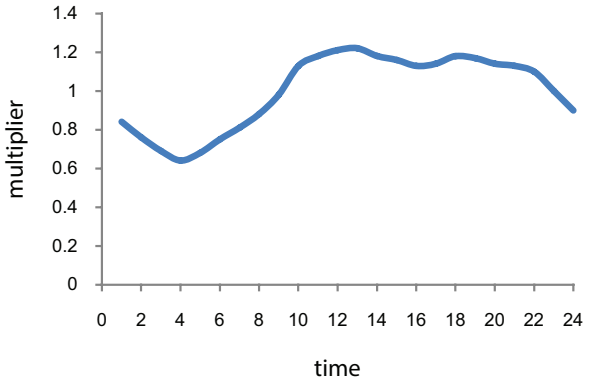

Fig. 2. Demand pattern coefficient of the real case study.

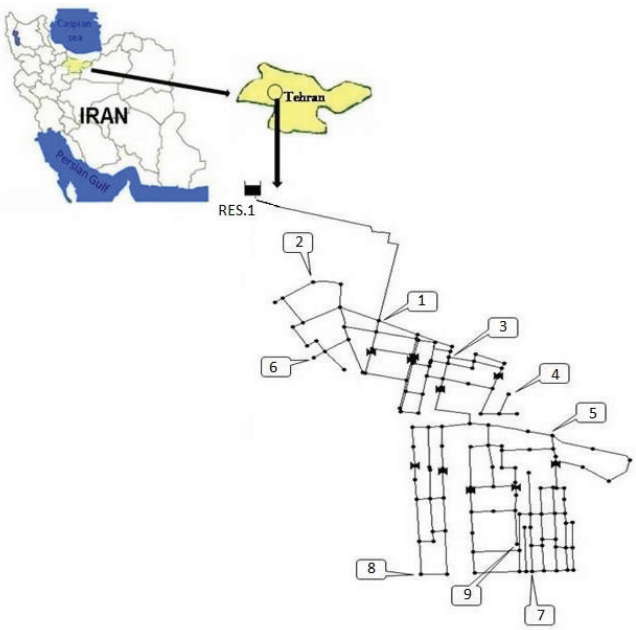

Fig. 3. Layout of the WDS model and location of pressure measurements.

4 months. The data loggers were placed at critical points in pressure variation to better identify system weaknesses to be considered in the improvement plans.

Because there are a large number of demand nodes and pipes of various diameters, ages (20–30 years) and materials, classification of pipes and nodes was useful. Network pipes were classified based on diameter, material and age as well as spatial distribution into nine classes. Each category of pipe had a unique Hazen–Williams coefficient (Fig. 4) that should be determined during calibration. Demand nodes were also classified into nine categories as shown in Fig. 5. The basis of node classification was the service area population density, land use and spatial distribution. The calibration parameter of each node shows the ratio of demand to average demand that was calculated based on per capita water demand and the population serviced by that node. It should be emphasized that especial attention should be paid to demand variations in nodes, before classification. There may be some nodes with very low or high water demands in a small region that should be taken into account.

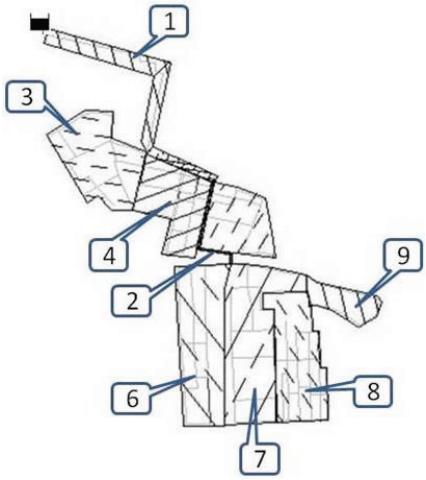

Fig. 4. The classification of WDN pipes into nine groups.

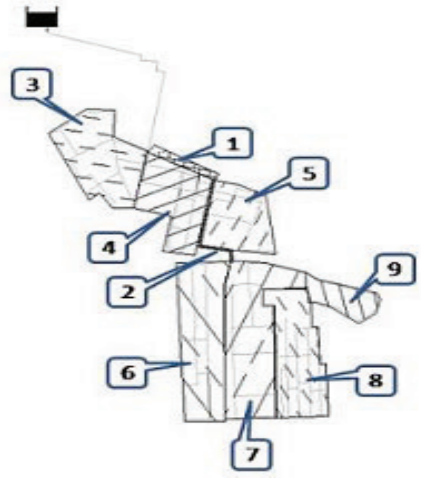

Fig. 5. The classification of demand nodes into nine groups.

Classification of pipes and nodes decreases the size of the decision space; therefore, the calibration model finds the desired answer easier and faster, which is desirable for practical applications. To avoid from unrealistic calibration results in the case study, the optimum Hazen–Williams coefficients were selected in a range of 0.15–1.3 times the initial value with an interval change of 0.1. For nodal demand, the search interval of optimal values were 0.1–1.2 times the initial value with a 0.002 change interval. A Pentium® Dual-Core CPU E5300 @ 2.60 GHz computer was used in this study. After running the model, various solutions with different fitness were produced. The smallest fitness value shows the most appropriate calibration results [33]. Because calibration results may be very similar, a dual check for results of calibration under different conditions was carried to determine the RMSE and NSE. The WDN was calibrated at 4, 7,10, 13, 16, 19,22 and 24 h over the course of 1 day based on the demand pattern. The different episodes for calibration of the nodal demand and Hazen–Williams coefficients as well as uncertainty in data measurements could produce different values for the variables for the same groups of components. Because a pipe cannot have several roughness coefficients over the course of a day, the results were aggregated by selecting the most repeated coefficient to provide the best result for calculation of the fitness function, NSE and RMSE in other episodes as follows:

$$C_{gi} = \text{mode}\,(C_{ti}) \tag{5}$$

where C_{gi} is selected Hazen–Williams coefficients in a group; C_{ti} is obtained Hazen–Williams coefficients at different times in a group 4.

Walski [34] found that WDN calibration will be acceptable if the difference between the pressure measurement and simulations is <5 m. In the present study, a maximum difference of 2 m was considered to be the threshold for acceptance of calibration results.

4. Results and discussion

4.1. Case study #1

Table 3 shows the calibrated and selected Hazen–Williams coefficients at different times in pipe groups 1 to 4. Table 4 compares the Hazen–Williams coefficients from Dini and Tabesh [27] and the proposed approach and indicates that the results are the same.

Table 5 shows the RMSE and NSE values at different hours of the day for simulated pressure after aggregation. The RMSE were <1 with a minimum of zero and a maximum of 0.67. The NSE values are close to 1 with a minimum of 0.9969. The results show the good performance of the proposed method. The total run time of the proposed method was 3 s per run and 24 s for all runs. The method proposed by Dini and Tabesh [27] required 9.70 min. This indicates the ability of the proposed method for application in real cases.

4.2. Case study #2

After sensitivity analysis of the parameters of the FMGA algorithm for a real network in this study, it was

Table 3
Hazen–Williams coefficients values at different times in pipe groups 1–4

Hazen–Williams coefficients values at different times										Selected option of Hazen–Williams coefficients
Grouping	Pipe	$t = 4$	$t = 7$	$t = 10$	$t = 13$	$t = 16$	$t = 18$	$t = 21$	$t = 22$	$t = 24$	
		C	C	C	C	C	C	C	C	C	C
Group 1	1	130	130	130	130	125	130	130	130	130	130
Group 2	2	85	85	75	80	75	80	77.67	80	80	80
Group 1	3	130	130	130	130	125	130	130	130	130	130
Group 3	4	70	70	75	70	70	70	71.38	70	70	70
Group 4	5	105	105	100	95	100	100	102.45	95	100	100
Group 2	6	85	85	75	80	75	80	77.67	80	80	80
Group 4	7	105	105	100	95	100	100	102.45	95	100	100
Group 3	8	70	70	75	70	70	70	71.38	70	70	70

Table 4
Comparison of Hazen–Williams coefficients from Dini and Tabesh [27] and the proposed approach

Pipe	Previous study	Current study (proposed approach)
1	130	130
2	80	80
3	130	130
4	70	70
5	100	100
6	80	80
7	100	100
8	70	70

Table 5
RMSE and NSE values at different hours of the day for simulated pressure after aggregation

Time	RMSE (m)	NSE
4	0.37	0.9983
7	0.49	0.9981
10	0.67	0.9969
13	0	1
16	0.33	0.9993
18	0.19	0.9998
21	0.06	1
22	0.05	1
24	0	1

concluded that the most important parameters were population size, cut, splice and mutation probabilities. Table 6 shows the results of sensitivity analysis at 4 am. As seen, for population sizes of 45, 95, 145, 190 and 225 in Table 6(A), the best fitness (0.031) was obtained from a population size of 145.

For a population size of 145, the cut probability increased gradually from 0.3% to 1.8% in Table 6(B). For this parameter, a value of <10% is desirable [31], and the best fitness was obtained at 1.5% cut probability.

A value of 50%–90% was desirable for optimal splice probability [31]. The best fitness value (0.031) was obtained at a splice probability of 90% (Table 6(C)).

The mutation is one of the most important GA operators. This study showed that the best result can be obtained in optimization process by only correct setting of this parameter. Usually, mutation probability is <10% [31], and in this study, its value was increased from 0.4% at first to 1.3% at the end. Finally, at 0.7% mutation probability, the fitness function reached its minimum value of 0.031 (Table 6(D)). Table 7 shows the summary of the best results for the optimization model parameters.

The results obtained in the first step of calibration for the different hours of the day are shown in Table 8. The five Hazen–Williams coefficient values selected for the different pipe groups are shown in the far right column of Table 8. For group 1, the Hazen-Williams coefficients were 117, 117, 119.6, 110.5, 119.6, 117, 117 and 110.5 at different times of day. The Hazen–Williams coefficient of 117 is repeated several times; therefore, it is assigned to this group. This process was repeated for the other groups, and the Hazen–Williams coefficients for remaining groups were 117, 99, 99.75, 99.75, 102.90, 94, 82, 98 and 70.

These values were replaced by the Hazen–Williams coefficients obtained from hourly calibration, and simulation was repeated for the same time periods. If the pressure difference was <2 m, ($P_{ji} \leq 2$ m) in all simulations, the values were considered to be acceptable; values that simulated pressures were considerably different from observations were replaced with the next most frequent coefficient and the simulation was repeated. This process was repeated until the criteria for pressure difference was satisfied.

Fig. 6 compares the observed and calibrated pressure after step one of calibration at 4, 7, 10, 13,16, 19, 22 and 24 h of the day. As shown, there was very good agreement between the calibrated and measured values.

Fig. 7 shows the observed pressure variations in pressure measurement points with simulation results before and after aggregation during a day. The results match well,

Table 6
The results of sensitivity analysis for real network at 4 am (A: population size, B: cut probability, C: splice probability, D: mutation)

	Trial										
	1,000	2,000	3,000	4,000	5,000	6,000	7,000	8,000	9,000	10,000	11,000
	Fitness	Fitness	Fitness	Fitness	Fitness	Fitness	Fitness	Fitness	Fitness	Fitness	Fitness
A: Population size											
45	0.143	0.143	0.117	0.061	0.044	0.043	0.043	0.043	0.040	0.040	0.040
95	0.178	0.074	0.074	0.045	0.037	0.037	0.037	0.037	0.037	0.037	0.037
145 (the best option)	0.194	0.156	0.061	0.036	0.032	0.031	0.031	0.031	0.031	0.031	0.031
190	0.143	0.143	0.143	0.102	0.071	0.049	0.044	0.044	0.043	0.036	0.036
225	0.143	0.143	0.127	0.072	0.072	0.043	0.037	0.032	0.032	0.031	0.031
B: Cut probability											
0.3	0.194	0.194	0.101	0.056	0.037	0.033	0.032	0.031	0.031	0.031	0.031
0.6	0.194	0.194	0.101	0.056	0.037	0.033	0.032	0.031	0.031	0.031	0.031
0.9	0.194	0.194	0.101	0.056	0.037	0.033	0.032	0.031	0.031	0.031	0.031
1.2	0.194	0.130	0.108	0.101	0.065	0.065	0.065	0.053	0.043	0.041	0.041
1.5 (the best option)	0.194	0.156	0.061	0.036	0.032	0.031	0.031	0.031	0.031	0.031	0.031
1.8	0.194	0.163	0.064	0.056	0.037	0.037	0.035	0.033	0.031	0.031	0.031
C: Splice probability											
50	0.194	0.166	0.100	0.096	0.045	0.045	0.034	0.032	0.030	0.030	0.030
60	0.194	0.142	0.088	0.088	0.065	0.053	0.036	0.032	0.031	0.030	0.031
70	0.194	0.194	0.126	0.102	0.085	0.085	0.085	0.054	0.044	0.037	0.037
80	0.194	0.163	0.103	0.099	0.064	0.064	0.064	0.042	0.040	0.034	0.034
90 (the best option)	0.194	0.156	0.061	0.036	0.032	0.031	0.031	0.031	0.031	0.031	0.031
D: Mutation											
0.4	0.194	0.133	0.107	0.105	0.067	0.067	0.067	0.041	0.033	0.031	0.031
0.7 (the best option)	0.194	0.156	0.061	0.036	0.032	0.031	0.031	0.031	0.031	0.031	0.031
1.0	0.194	0.136	0.088	0.049	0.037	0.036	0.035	0.033	0.031	0.031	0.031
1.3	0.194	0.134	0.072	0.039	0.036	0.033	0.031	0.031	0.031	0.031	0.031

Table 7
The summary of the best results for the optimization model parameters (real network)

Parameter	Best value	Trial	Fitness
Population size	145	6,000	0.031
Cut probability	1.5	6,000	0.031
Splice probability	90	6,000	0.031
Mutation	0.7	6,000	0.031

and the proposed algorithm was able to preserve system performance.

Table 9 shows the calibrated demand after aggregation at pressure measurement points for 4, 7, 10, 13, 16, 19, 22 and 24 h. The results of calibration were evaluated at different hours of the day.

Table 10 shows the RMSE and NSE at different hours of the day for pressure simulation after aggregation. Table 10 shows that the RMSE was always <1 with a minimum value of 0.26 and a maximum value of 0.74. The NSE approached 1 with a minimum value of 0.9954 and a maximum value of 0.9994.

Local standards [35] set the maximum allowable pressure for WDSs at 50 m. Under certain circumstances and if the topographic conditions result in significant cost, the maximum allowable pressure can be increased to 60 m. The minimum pressure for the water demand supply of a 4-story building is 26 m. Local measurements showed that when the pressure drops to below 10 m, no water can be supplied because of head loss in the home piping system and flow meter equipment. If the node pressure is <10 m, the network is in a no-service state. Using these pressure limitations, four classes of system performance were developed as shown in Table 11 as the percentages for nodes in different classes before and after calibration at different hours of the day. It can be concluded that if the system was simulated based on the initial assumptions about the calibration variables, the results of the performance evaluation and, therefore, modification plans would differ. This illustrates the strong importance

Table 8
Hazen–Williams coefficients values at different times in groups of 1–9

Hazen–Williams coefficients values at different hours									Selected options of Hazen– Williams coefficients				
Group name	$t = 4$	$t = 7$	$t = 10$	$t = 13$	$t = 16$	$t = 19$	$t = 22$	$t = 24$	1	2	3	4	5 (the best option)
	C	*C*	*C*	*C*	*C*	*C*	*C*	*C*	*C*	*C*	*C*	*C*	*C*
Group 1	117.0	117.0	119.6	110.5	119.6	117.0	117.0	110.5	117.0	117.00	117.0	117.00	117.00
Group 2	90.00	90.00	99.00	85.00	99.00	98.00	110.00	102.00	90.00	99.00	99.00	99.00	99.00
Group 3	90.30	100.80	99.75	89.25	99.75	108.15	94.50	96.60	99.75	99.75	99.75	99.75	99.75
Group 4	94.50	115.50	99.75	89.25	99.75	108.15	94.50	96.60	94.50	94.50	99.75	99.75	99.75
Group 5	102.90	113.40	97.65	89.25	97.65	108.15	94.50	98.70	97.65	98.70	108.15	113.40	102.90
Group 6	83.00	93.00	94.00	85.00	94.00	98.00	100.00	70.00	94.00	85.00	83.00	98.00	94.00
Group 7	82.00	82.00	104.00	85.00	94.00	103.00	90.00	80.00	82.00	85.00	94.00	90.00	82.00
Group 8	101.00	98.00	91.00	85.00	91.00	98.00	90.00	90.00	90.00	91.00	98.00	98.00	98.00
Group 9	92.00	105.00	104.00	102.00	104.00	103.00	90.00	70.00	104.00	92.00	90.00	90.00	70.00

Table 9
Calibrated demand after aggregation at pressure measurement points at different hours

Measurement points	4 am	7 am	10 am	1 pm	4 pm	7 pm	10 pm	12 am
	Demand (L/s)	Demand (L/s)	Demand (L/s)	Demand (L/s)	Demand (L/s)	Demand (L/s)	Demand (L/s)	Demand (L/s)
1	2.16	2.79	3.78	4.29	3.73	4.12	3.85	2.35
2	2.10	3.12	3.85	3.73	3.82	4.03	3.86	3.57
3	2.50	3.23	4.38	4.80	4.32	0.44	4.46	3.93
4	1.74	1.18	3.04	3.44	2.99	3.36	2.94	2.72
5	2.26	2.91	3.95	4.25	3.89	3.99	4.13	1.93
6	2.41	3.58	4.96	4.71	4.89	5.44	4.98	4.33
7	2.17	2.99	4.00	3.44	3.83	4.05	3.45	3.41
8	2.60	3.35	4.55	5.16	4.49	4.60	4.85	3.12
9	2.59	3.34	3.96	5.14	4.47	4.58	3.42	3.27

Table 10
The values of RMSE and NSE at different hours of the day to simulate of pressure

Time	RMSE (m)	NSE
4	0.49	0.9972
7	0.59	0.9959
10	0.26	0.9994
13	0.74	0.9954
16	0.37	0.9989
19	0.33	0.9992
22	0.38	0.9988
24	0.41	0.9985

of calibration. The proposed scheme allows calibration more quickly with more desirable operation. Water quality in WDN can also be assessed by fuzzy logic methods [36].

5. Conclusions

The Hazen–Williams coefficients and nodal demand were calibrated over the course of 1 day using WaterGEMS simulator and FMGA using the new approach of aggregation. The objective function was to minimize the square of the difference between the measured and simulated values. The Hazen–Williams coefficients and nodal demand were the decision variables.

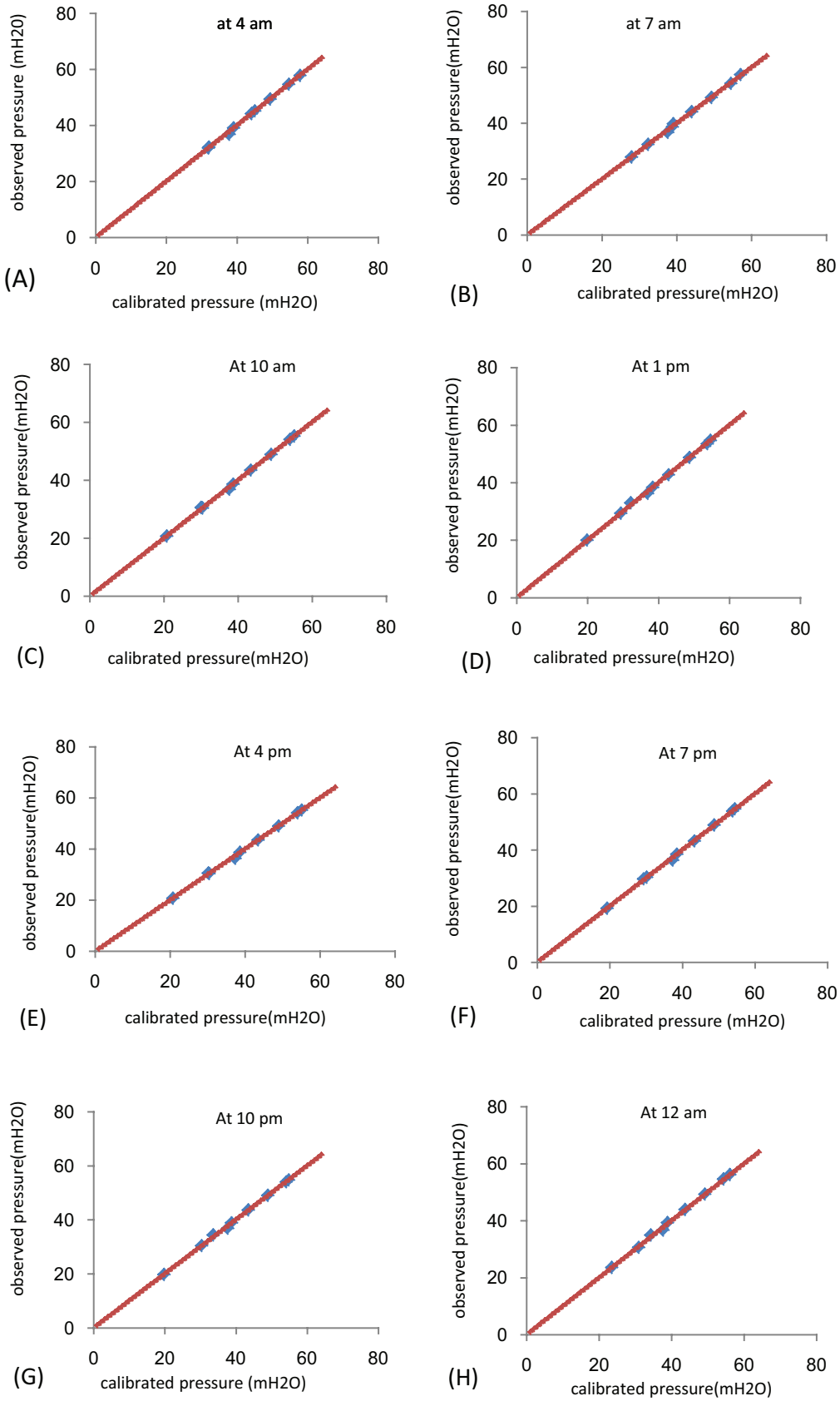

Fig. 6. Comparison of the observed and calibrated pressures after the first step of calibration in different times in a day.

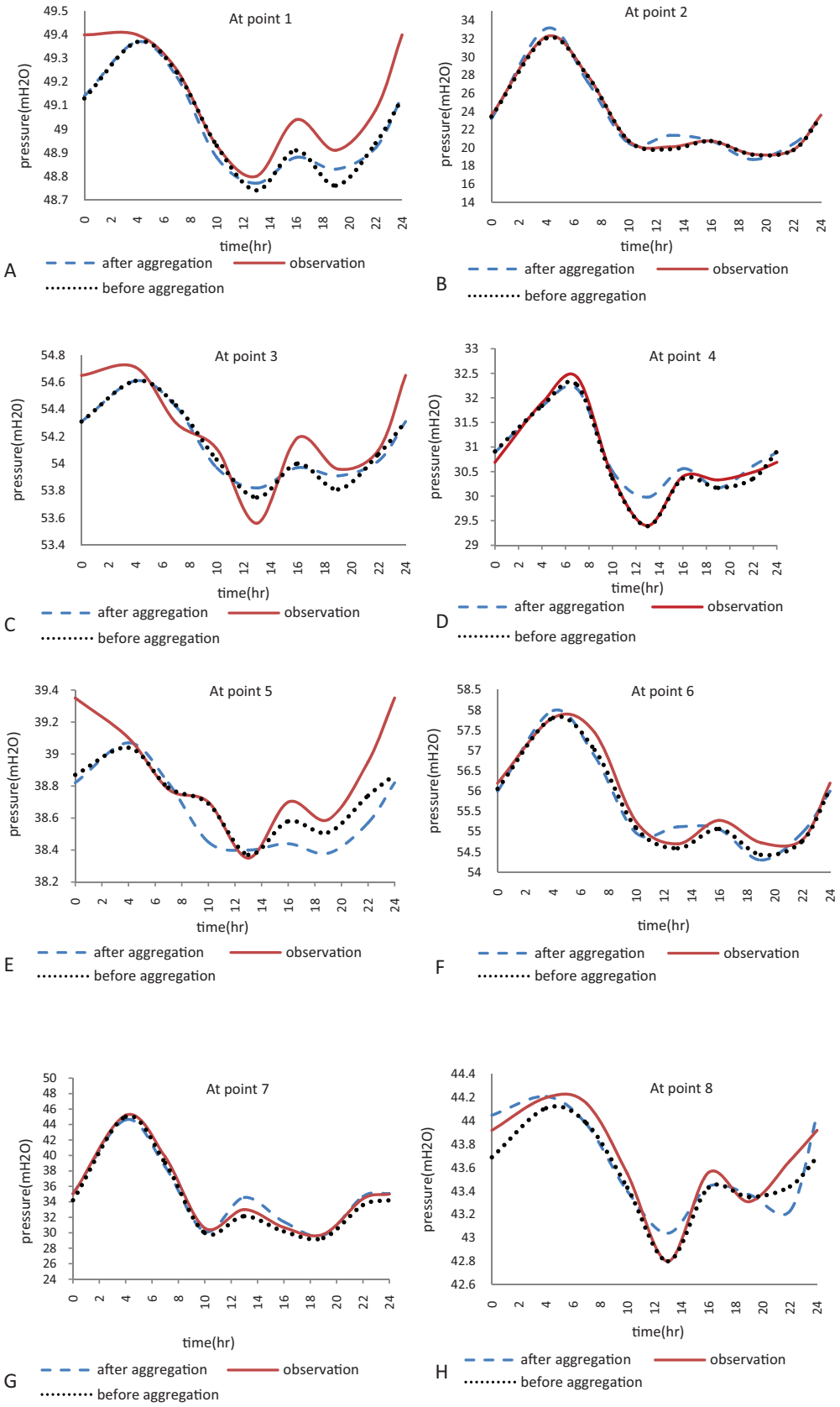

Fig. 7. Comparison of the observed pressure variations in pressure measurement points with simulation results before and after aggregation during a day.

Table 11
The change percentage of output pressure in the software before and after aggregation

Time	Pressure	Lack of servicing	Lack of servicing to acceptable	Acceptable to good	Good to desired	Desired to good	Good to acceptable	Acceptable to unacceptable	Unacceptable
		<10	10–26	26–28.5	28.5–31	31–38	38–50	50–60	>60
$t = 4$	Initial	–	0.73	6.57	1.46	18.25	38.69	27.74	6.57
	Aggregation	–	0.73	6.57	1.46	18.98	38.69	27.01	6.57
$t = 7$	Initial	–	0.73	8.03	4.38	18.25	36.50	25.55	6.57
	Aggregation	–	2.19	8.03	5.11	23.36	29.20	26.28	5.84
$t = 10$	Initial	–	7.30	8.03	6.57	24.09	24.82	24.09	5.11
	Aggregation	–	8.76	8.76	7.30	21.90	24.09	24.09	5.11
$t = 13$	Initial	–	8.76	10.22	8.03	19.71	24.09	24.09	5.11
	Aggregation	–	6.57	8.03	5.11	24.82	27.01	24.09	4.38
$t = 16$	Initial	–	7.30	8.03	6.57	24.09	24.82	24.09	5.11
	Aggregation	–	7.30	8.03	8.03	22.63	24.82	24.09	5.11
$t = 19$	Initial	–	8.76	8.03	8.03	21.90	24.09	24.09	5.11
	Aggregation	–	8.76	8.76	9.49	20.44	24.09	23.36	5.11
$t = 22$	Initial	–	8.76	8.03	8.03	21.90	24.09	24.09	5.11
	Aggregation	–	6.57	8.03	2.92	26.28	27.01	24.09	5.11
$t = 24$	Initial	–	2.19	9.49	3.65	23.36	29.20	26.28	5.84
	Aggregation	–	6.57	8.03	2.92	24.09	27.74	24.82	5.84

In this new approach, the 24-h day was divided into some hourly calibration to reduce the number of calculations and the time needed to reach an optimal solution. Each unit was optimized separately, and the results aggregated to achieve an optimal solution to minimize error. In previous studies, the high volume of calculations and time consumed for calibration of average demand and the demand variability was ignored. In the proposed approach, all hours of the day are considered in calibration easily; thus, the network can be modified using the optimal calibration coefficients. The results of the proposed method on a benchmark example showed that the Hazen–Williams coefficients obtained were identical to results of previous studies. In addition, the time required to reach an optimal solution using aggregation was much less than for previous methods.

References

[1] M. Tabesh, M. Jamasb, R. Moeini, Calibration of water distribution hydraulic models: a comparison between pressure dependent and demand driven analyses, Urban Water J., 8 (2011) 93–102.

[2] V. Kanakoudis, K. Gonelas, Assessing the results of a virtual pressure management project applied in Kos Town water distribution network, Desal. Wat. Treat., 57 (2016) 11472–11483.

[3] F. Di Pierro, S.-T. Khu, D. Savić, L. Berardi, Efficient multi-objective optimal design of water distribution networks on a budget of simulations using hybrid algorithms, Environ. Modell. Software, 24 (2009) 202–213.

[4] D.A. Savic, G.A. Walters, Genetic algorithms for least-cost design of water distribution networks, J. Water Resour. Plann. Manage., 123 (1997) 67–77.

[5] K. Vairavamoorthy, M. Ali, Optimal design of water distribution systems using genetic algorithms, Comput.-Aided Civ. Infrastruct. Eng., 15 (2000) 374–382.

[6] K. Vairavamoorthy, M. Ali, Pipe index vector: a method to improve genetic-algorithm-based pipe optimization, J. Hydraul. Eng., 131 (2005) 1117–1125.

[7] M.d.C. Cunha, J. Sousa, Water distribution network design optimization: simulated annealing approach, J. Water Resour. Plann. Manage., 125 (1999) 215–221.

[8] A.C. Zecchin, A.R. Simpson, H.R. Maier, M. Leonard, A.J. Roberts, M.J. Berrisford, Application of two ant colony optimisation algorithms to water distribution system optimisation, Math. Comput. Modell., 44 (2006) 451–468.

[9] Z. Geem, J.H. Kim, G. Loganathan, Harmony search optimization: application to pipe network design, Int. J. Model. Simul., 22 (2002) 125–133.

[10] Z.W. Geem, Optimal cost design of water distribution networks using harmony search, Eng. Optim., 38 (2006) 259–277.

[11] M.M. Eusuff, K.E. Lansey, Optimization of water distribution network design using the shuffled frog leaping algorithm, J. Water Resour. Plann. Manage., 129 (2003) 210–225.

[12] M.D. Lin, Y.-H. Liu, G.-F. Liu, C.-W. Chu, Scatter search heuristic for least-cost design of water distribution networks, Eng. Optim., 39 (2007) 857–876.

[13] N. Ghajarnia, O. Bozorg Haddad, M.A. Mariño, Performance of a novel hybrid algorithm in the design of water networks, Proc. Inst. Civil Eng. Water Manage., 164 (2011) 173–191.

[14] L.E. Ormsbee, D.J. Wood, Explicit pipe network calibration, J. Water Resour. Plann. Manage., 112 (1986) 166–182.

[15] S.M. Kumar, S. Narasimhan, S.M. Bhallamudi, Parameter estimation in water distribution networks, Water Resour. Manage., 24 (2010) 1251–1272.

[16] Z. Weiwei, Y. Guoping, S. Shihu, Notice of Retraction Calibration of Pipe Roughness Coefficients under Multiple Loading Conditions by Real-coded Genetic Algorithm, 2010 International Conference on Computer Application and System Modeling (ICCASM), IEEE, 2010, pp. V12-588–V512-592.

[17] A. Borzì, E. Gerbino, S. Bovis, M. Corradini, Genetic Algorithms for Water Distribution Network Calibration: A Real Application, Proc. 8th International Conference on Computing and Control for the Water Industry, University of Exeter, UK, 2005, pp. 149–154.

[18] Z. Yu, Y. Tian, Y. Zheng, X. Zhao, Calibration of pipe roughness coefficient based on manning formula and genetic algorithm, Trans. Tianjin Univ., 15 (2009) 452–456.
[19] M. Jamasb, M. Tabesh, M. Rahimi, Calibration of EPANET Using Genetic Algorithm, Proc. Water Distribution Systems Analysis, Kruger National Park, South Africa, 2009, pp. 17–20.
[20] D. Kang, K. Lansey, Demand and roughness estimation in water distribution systems, J. Water Resour. Plann. Manage., 137 (2010) 20–30.
[21] W. Cheng, Z. He, Calibration of nodal demand in water distribution systems, J. Water Resour. Plann. Manage., 137 (2010) 31–40.
[22] M. Asadzadeh, B.A. Tolson, R. McKillop, A Two Stage Optimization Approach for Calibrating Water Distribution Systems, Proc. 12th Water Distribution Systems Analysis, ASCE, Reston, VA, 2010.
[23] G. Sanz, R. Pérez, Demand pattern calibration in water distribution networks, Procedia Eng., 70 (2014) 1495–1504.
[24] A.F. Morosini, P. Veltri, F. Costanzo, D. Savić, Identification of leakages by calibration of WDS models, Procedia Eng., 70 (2014) 660–667.
[25] D. Kang, K. Lansey, Demand and roughness estimation in water distribution systems, J. Water Resour. Plann. Manage., 137 (2011) 20–30.
[26] M. Dini, Quality Based Optimal Renovation Planning for Water Distribution Networks Considering Reliability Indices, PhD Thesis, University of Tehran, College of Engineering, School of Civil Engineering, Iran, 2014.
[27] M. Dini, M. Tabesh, A new method for simultaneous calibration of demand pattern and Hazen-Williams coefficients in water distribution systems, Water Resour. Manage., 28 (2014) 2021–2034.
[28] Haested Methods, WaterGEMS User's Guide, Bentley Systems, Incorporated, Haested Methods Solution Center, Watertown, CT, USA, 2005.
[29] Z. Wu, Q. Wang, S. Butala, T. Mi, Y. Song, Darwin Optimization Framework User Manual, Bentley Systems, Incorporated, Watertown, CT, USA, 2012.
[30] D.E. Goldberg, K. Deb, H. Kargupta, G.R. Harik, Rapid, Accurate Optimization of Difficult Problems Using Fast Messy Genetic Algorithms, Proc. 5th International Conference on Genetic Algorithms, 1993, pp. 56–64.
[31] A. Haghighi, E. Bakhshipour, Optimization of Sewer Networks Using an Adaptive Genetic Algorithm, Water Resour. Manage., 26 (2012) 3441–3456.
[32] E. Alperovits, U. Shamir, Design of optimal water distribution systems, J. Water Resour. Res., 13 (1977) 885–900.
[33] Z.Y. Wu, T. Walski, R. Mankowski, G. Herrin, R. Gurrieri, M. Tryby, Calibrating Water Distribution Model via Genetic Algorithms, Proc. AWWA IMTech, Kansas, Mo, 2002.
[34] T.M. Walski, Technique for calibrating network models, J. Water Resour. Plann. Manage., 109 (1983) 360–372.
[35] Islamic Republic of Iran Vice Presidency for Strategic Planning and Supervision, Design Criteria of Urban and Rural Water Supply and Distribution Systems, No. 117–3, 2013 (in Farsi).
[36] H. Gharibi, A.H. Mahvi, R. Nabizadeh, H. Arabalibeik, M. Yunesian, M.H. Sowlat, A novel approach in water quality assessment based on fuzzy logic, J. Environ. Manage., 112 (2002) 87–95.